

PHOTON STRUCTURE

Jacek Turnau for the H1 and ZEUS Collaborations¹
 H. Niewodniczanski Institute of Nuclear Physics, Krakow
 Kawory 26a 30-055 Krakow e-mail jacek.turnau@ifj.edu.pl

Abstract

Measurements of di-jet production at HERA provide an important test of NLO QCD calculations. It is also a source of information about the partonic content of the photon, complementary to the measurements in e^+e^- experiments. In this article we review the status of the photon structure studies with particular emphasis on HERA measurements.

1 Introduction

The HERA collider, where 27.5 GeV positrons collide with 820/920 GeV protons, is traditionally considered as a natural extension of Rutherford's experiment and the process of deep inelastic scattering (ep DIS) is interpreted as a reaction in which a virtual photon, radiated by the incoming positron, probes the structure of the proton. However, there are regions of phase space for ep collisions where it is other way round: where partons in the proton probe the photon structure.

The structure of the talk will be the following: it will start with posing the problem i.e. a description of our understanding of the structure of the photon in terms of Quantum Field Theory (QFT) and the motivations for its investigation. Next, we briefly review measurements of the photon structure in e^+e^- experiments and its general properties. In the main part, we review HERA measurements sensitive to the structure of the photon. We end with a summary and conclusions.

Various aspects of the subject discussed here have been covered recently in many excellent review articles e.g. [1], [2], [3], [4].

2 Structure or interaction dynamics?

The photon is the gauge boson of QED and, as far as we know, elementary. In any QFT the existence of the interaction means also that the quanta themselves have structure. Coupling between field quanta will make possible fluctuations, or splitting of any quantum over limited time, into two (or more in higher order) quanta. For example in QED a photon can fluctuate into an electron-positron (e^+e^-) pair, or, as first noted by Ioffe [7], into a $q\bar{q}$ pair. If the fluctuation time defined in the probing objects rest frame as $t_f \approx 2E_\gamma/m_{q\bar{q}}^2$ is much larger than the interaction time t_{int} , the photon builds up structure in the interaction. Here, E_γ is the energy of the fluctuating photon and $m_{q\bar{q}}$ is the mass into which it fluctuates. The fluctuation time of a photon with virtuality Q^2 is given by $t_f \approx 2E_\gamma/(m_{q\bar{q}}^2 + Q^2)$, and thus at very high Q^2 one does not expect the condition $t_f \gg t_{int}$, unless the probe has even higher virtuality.

It is clear that what we described here as the photon structure is a part of the interaction dynamics. In practice in any high energy interaction, the distinction between structure and interaction is determined by the factorisation scale. This is a momentum transfer squared scale below which any parton activity is considered to be part of the parent structure and above which any parton activity is considered to be a part of the interaction dynamics. It is exactly in this sense that in ep DIS we measure the proton structure function $F_2(x, Q^2)$ at a factorisation (or resolution) scale Q^2 : Q^2 is almost always the largest momentum transfer squared scale in DIS, so all parton activity at lower transverse momenta should be associated with the target i.e. proton. The structure function is interpreted as a density of quarks and antiquarks which carry a fraction x of the proton momentum. Any structure function is thus dependent on the choice of the factorisation (resolution) scale. It was shown that structure functions for hadrons can be used universally in any high energy interaction at a given scale. In the same way it is also expected that photon structure $F_2^\gamma(x_\gamma, Q^2)$ will be similarly universal and factorisable.

When interactions are switched off the photon remains structureless so we say that photon structure is driven by fluctuations. It is in many respects different from that of hadrons which have structure even

¹To be published in Proceedings of the Workshop on Quantum Field Theory and High Energy Physics Tver 2000, Work partially supported by Polish Committee for Scientific Research grant 2P03B10318.

after interactions are switched off (valence driven structure). In addition, the photon structure can be investigated as a function of its virtuality i.e. size, which is not possible for hadrons. We have thus several strong motivations for the photon structure studies:

- Measurements of the photon structure function provide interesting tests of QCD. Some pose even a challenge to theory e.g. there is no full theory of the parton density suppression due to increasing virtuality (only an asymptotic prediction exists)
- The parametrisation of the universal and factorisable photon structure function based on LEP and HERA measurements is a necessary component of the description of many high energy processes
- At future linear colliders it will be very important to understand the large number of events from photon interactions. Some photon interactions can be important probes to look for new physics, for example the production of Higgs bosons at a photon linear collider ($\gamma\gamma \rightarrow H$) [6].

3 Photon structure from e^+e^- and its general properties

The hadronic structure of the photon can be probed either by virtual photons in e^+e^- collisions or by virtual partons in ep collisions at HERA. This article is devoted mainly to the recent measurements at the HERA collider, but for the sake of completeness some e^+e^- results are discussed in this section.

The principle of the measurement of the hadronic structure function of the photon $F_2^\gamma(x_\gamma, Q^2)$ is depicted in Figure 1 (left). A highly virtual γ^* with large $Q^2 = -q^2$ probes a quasi-real γ with virtuality $P^2 \approx 0$. In this measurement the energy of the target is not known so x_γ (the fraction of the photon momentum carried by the interacting parton) has to be reconstructed from the hadronic final state. This leads to systematic uncertainties and a limited reach for small values of x_γ . To underline the analogies and differences we depict the principle of the measurement of the proton structure function on the right of Figure 1.

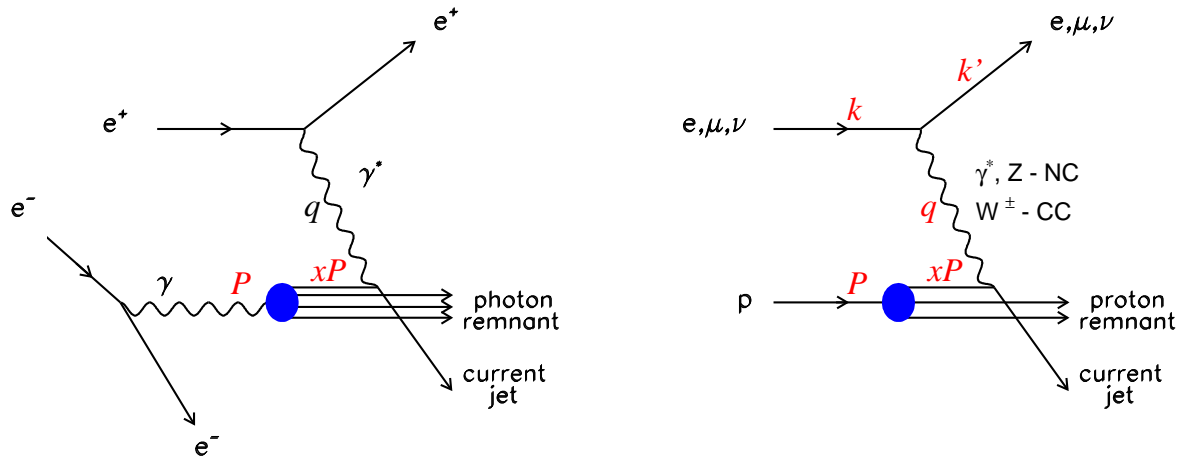


Figure 1: A diagram (left) describing the process of deep inelastic scattering of a positron on a quasi-real γ using the reaction $e^+e^- \rightarrow e^+e^-X$. The four-vector of the virtual γ (probe) is q , the four momentum of the struck quark is xP . To underline the analogy with the measurement of the hadronic structure function, a diagram describing lepton-proton deep inelastic scattering is shown in the right diagram.

Many measurements of the hadronic structure function of the photon have been performed at several e^+e^- colliders. The range of resolution scale covered by various experiments is $0.24 \leq \langle Q^2 \rangle \leq 700 \text{ GeV}^2$. In Figure 2 we present a compilation [3] (recently updated with OPAL data [5]) of photon structure function measurements in various e^+e^- experiments. F_2^γ is plotted as a function of Q^2 for several ranges of x_γ . One can see positive scaling violation for all x_γ . This is the most striking feature of the photon structure in comparison to the structure of the proton, for which positive scaling violation is observed

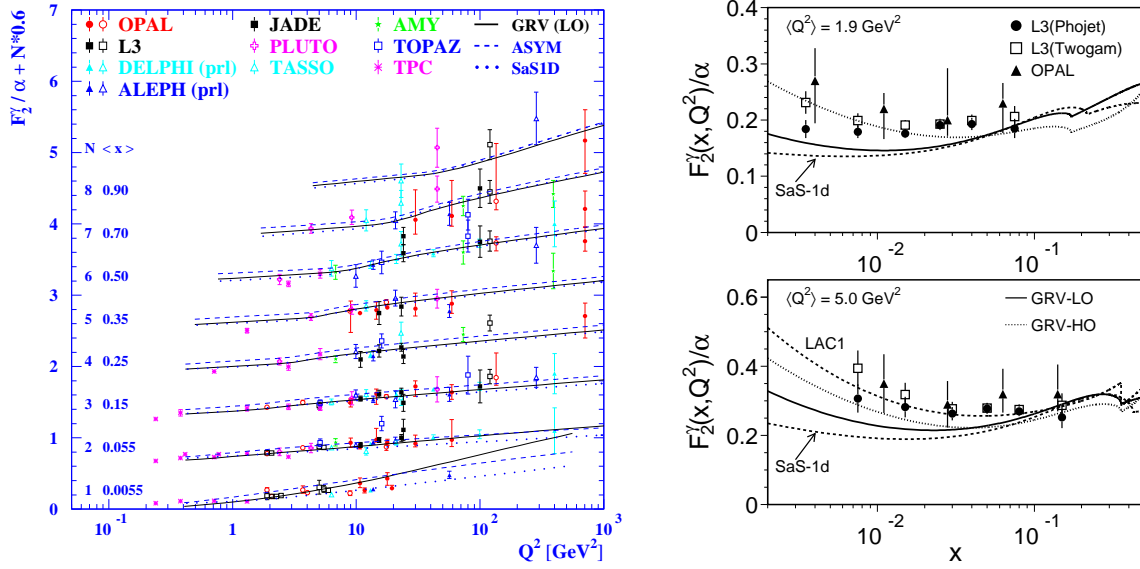


Figure 2: *Left:* The photon structure function F_2^γ , as a function of Q^2 , for average x values as given in the figure. The curves are the expectations of different parametrisations of parton distributions in the photon. *Right:* The photon structure as a function of the photon momentum fraction x at fixed resolution scale Q^2 . The curves are different parametrisations of parton distributions in the photon.

only at low x values. This different behavior can be understood in terms of perturbative QCD as coming from the splitting $\gamma \rightarrow q\bar{q}$, having no analogue in the proton case. In addition, and again contrary to the proton case, it also causes the photon structure function to be large for high x values.

A simple LO parametrisation of the photon structure function

$$F_2^\gamma = 3 \sum_q e_q^4 \frac{\alpha}{\pi} x [x^2 + (1-x)^2] \ln \frac{Q^2}{\Lambda^2} + [\text{hadron}' \equiv \text{VDM}] \quad (1)$$

can be written down in QCD. The expression is asymptotic i.e. all terms not multiplied by large $\ln Q^2$ are dropped. The second term in the equation – “hadron” part, corresponds to $\gamma \rightarrow q\bar{q}$ fluctuations with virtuality below a cutoff value Λ^2 . This noncalculable piece is traditionally represented by photon fluctuations into vector mesons, as proposed 30 years ago in terms of the Vector Dominance Model [8]. Witten [9] and others showed that the above mentioned features of the LO formula (1) remain valid in calculations which include higher order perturbative terms. Thus a rising dependence of F_2^γ with increasing probe scale Q^2 throughout most of the range of x is thereby seen to be a characteristic feature of the “fluctuation driven” (rather than “valence driven”) structure functions. Measurements compiled in Figure 2 provide therefore an interesting and important test of pQCD.

Since the measurements of F_2^γ span a wide range of Q^2 , it is possible to apply the DGLAP pQCD formalism [10] as is done for the proton structure function. As a result parton density functions (pdfs) for the photon are available.

There exist several pdfs for real and also for virtual photons in leading and next-to-leading order, which are based on the full evolution equations. They are constructed in manner very similar to that for the proton pdfs. They differ in the assumptions made about the starting scale, the input distributions assumed at this scale and also in the amount of data used in fitting their parameters. Those most quoted in the literature are LAC [11], GRV [12], AGF [13] and SAS [14]. These parametrisations were developed before the publication of the new LEP data. LEP has measured the photon structure function F_2^γ in the range $0.002 \leq x_\gamma \leq 1.0$ and $1.86 < \langle Q^2 \rangle < 700$ GeV². These data represent an important step in the reduction of statistical and systematic uncertainties and cover a larger kinematic region both in x_γ and Q^2 . From Figure 2 (right) it is clear that the LEP data provide new information on photon structure

and the existing pdf parametrisations will have to be revisited.

4 Photon structure from HERA

At HERA the photon structure is investigated mainly by measurements of high E_T jets and charged particles [16]-[23]. The partonic structure of quasi-real or virtual target photons is probed by a parton from the proton producing a pair of partons of large transverse momentum squared E_T^2 much larger than the photon virtuality Q^2 . Due to the large cross section at HERA the photon can be probed at even larger factorisation scales than at LEP.

The photoproduction of jets through a hard parton differs from the jet production in hadron-hadron collisions in one respect: the photon interacts either by means of its direct coupling to high E_T partons or by means of partons in its structure, which are resolved in the interaction. This is depicted in Figure 3.

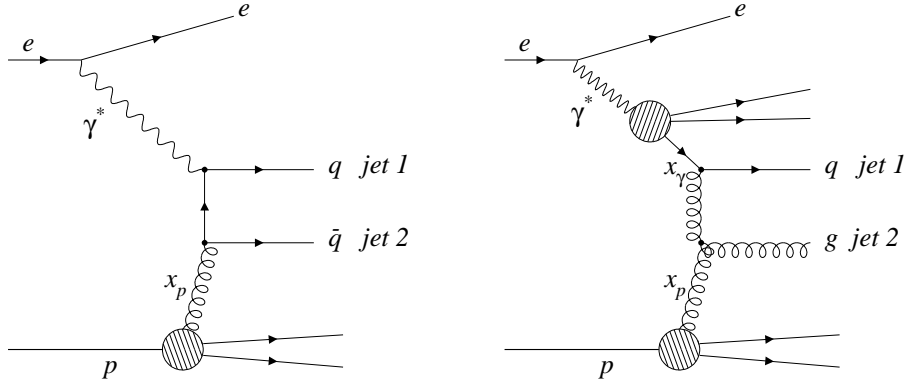


Figure 3: A diagram (left) describing the direct process of di-jet production in LO. The photon couples directly to high E_T partons. The diagram on the right depicts the resolved di-jet production in LO. The photon interacts through partons belonging to its structure which carry x_γ fraction of its momentum.

The terminology “direct” and “resolved” processes is now established, though in reality the direct photon contains fluctuation driven structure not resolved at a given scale.

The fraction of the photon momentum carried by an interacting parton can be reconstructed at hadron level from jet kinematics

$$x_\gamma^{jet} = \sum_{jets} \frac{E_{T,jet} e^{-\eta_{jet}}}{E_\gamma} \quad (2)$$

where $E_{T,jet}$ and η_{jet} are the transverse jet energy and pseudorapidity of the jets. The sum extends over high E_T jets (i.e. does not include the photon and proton remnant jets). The “true” (i.e. parton level) fraction x_γ can be unfolded from the data using simulated $x_\gamma - x_\gamma^{jet}$ correlations. In order to reach low values of x_γ the measurement should extend to low values of the jet transverse momentum and/or high values of their pseudorapidity (i.e. close to the proton remnant). Both requirements are experimentally challenging. In particular, the low cut on E_T results in large corrections for hadronisation and soft underlying events i.e. secondary interactions of the partons belonging to the photon and proton remnants.

In the LO QCD approximation to di-jet photoproduction, the ep cross section is written

$$\frac{d^5\sigma}{dy dx_\gamma dx_p d\cos\theta^* dQ^2} = \frac{1}{32\pi s_{ep}} \frac{f_{\gamma/e}(y, Q^2)}{y} \sum_{ij} \frac{f_{i/\gamma}(x_\gamma, E_T^2, Q^2)}{x_\gamma} \frac{f_{j/p}(x_p, E_T^2)}{x_p} |M_{ij}(\cos\theta^*)|^2 \quad (3)$$

where $f_{i/\gamma}$ and $f_{i/p}$ are the pdfs for each parton species i in a photon and a proton, respectively. They are evaluated at the factorisation scale E_T^2 . The M_{ij} are QCD matrix elements for $2 \rightarrow 2$ parton-parton

hard scattering processes. The quantity s_{ep} is the square of the centre of mass energy in the ep collision, and θ^* is the polar angle of the outgoing partons in the parton-parton centre of mass frame.

The measurement of the di-jet cross section can be exploited to gain information about the parton densities in the photon. There are two conceptually different approaches, which can be nicknamed “extraction” and “universality test”.

We can extract the parton density in the photon treating the measured di-jet cross section, the parton density in the proton (well constrained by inclusive ep DIS data) and the QCD matrix element as input to formula (3). The result of the measurement is a fundamental, parton level quantity. This approach has one important limitation: it is the LO procedure, because it employs the LO notion of the effective parton density and the LO Monte Carlo which relates parton to hadron levels. The H1 collaboration extracted the parton density in photon in the region of the low x_γ where gluon component of the parton density is of particular interest and poorly constrained by e^+e^- measurements.

In the “universality test” we have different objective: to check if the parametrisation of parton density in photon constrained by e^+e^- measurements is adequate for the description of the inclusive di-jet cross section within NLO QCD theory. In this approach one of the existing parametrisations of the parton density in photon [11]-[14] is used as input information in the NLO calculation [24] of jet photoproduction cross section at the parton level. In order to be consistent, we have to avoid the application of the LO Monte Carlo for hadronic and soft underlying event corrections and thus restrict the analysis to the region where these corrections are expected to be small: high transverse jet energy hence high x_γ (see formula (2)). The calculated parton level cross sections are compared with the data at the hadron level, which means that the data are corrected for detector effects only.

It should be underlined that neither approach is satisfactory, especially at the level of the measurement precision recently reached by both HERA experiments. Tools for extraction of the NLO pdf in photons from di-jet measurements, similar to those existing for the proton pdf, are missing. Obviously, there are important technical differences between electromagnetic and strong probes: in the case of ep or $e\gamma$ DIS the resolution scale does not have to be unfolded for hadronisation and other QCD effects, because it is known directly from the electron measurement. In addition, the strong probe comes in two species (quark or gluon), and this certainly complicates the fitting procedure. The LO solution to this problem, i.e. Single Effective Parton Density approach (see sec. 4.1), may be not applicable in NLO theory.

4.1 Measurement of the Effective Parton Density of quasi-real photons

At HERA we cannot distinguish experimentally which partons initiated the hard scattering process in Figure 3, therefore formula (3) is not suitable for the extraction of parton densities. To avoid this difficulty, the H1 Collaboration adopted the Single Effective Subprocess (SES) approximation [25], which exploits the fact that the dominant contributions to the cross section come from the parton-parton scattering matrix elements which have similar shapes. Introducing the effective pdf in the photon

$$f_\gamma^{\text{eff}}(x_\gamma, E_T^2) \equiv \sum_{n_f} (f_{q/\gamma}(x_\gamma, E_T^2) + f_{\bar{q}/\gamma}(x_\gamma, E_T^2)) + \frac{9}{4} f_{g/\gamma}(x_\gamma, E_T^2), \quad (4)$$

the effective proton pdf f_p^{eff} and the SES matrix element M_{SES} , we can express the resolved photon contribution to the cross section by the product $f_\gamma^{\text{eff}} f_p^{\text{eff}} |M_{\text{SES}}|^2$. As f_p^{eff} is well constrained by the data and M_{SES} is calculable in perturbative QCD, f_γ^{eff} can be directly determined from the measurement of the di-parton cross section.

In Figure 4 (left) we show the H1 measurement [18] of the di-jet cross section as a function of the parton momentum fraction x_γ^{jet} .

The histograms represent a LO QCD MC calculation showing the contributions of the direct photon-proton interactions as well as the quark and gluon induced processes using the GRV pdfs for photon and proton. It should be noted that the relatively low cut on the jet transverse energy ($E_T^{\text{jets}} > 6$ GeV) allows a precise measurement down to $x_\gamma = 0.05$. Sensitivity to the gluon content of the photon is clearly seen. In the definition of $d\sigma/dx_\gamma^{\text{jet}}$ pedestal of the jet transverse momentum due to the soft underlying event is subtracted. This is carefully checked by comparing the energy flow around the jets in data and simulation which agrees very well. The remaining differences are added to the systematic errors. In Figure 4 (right)

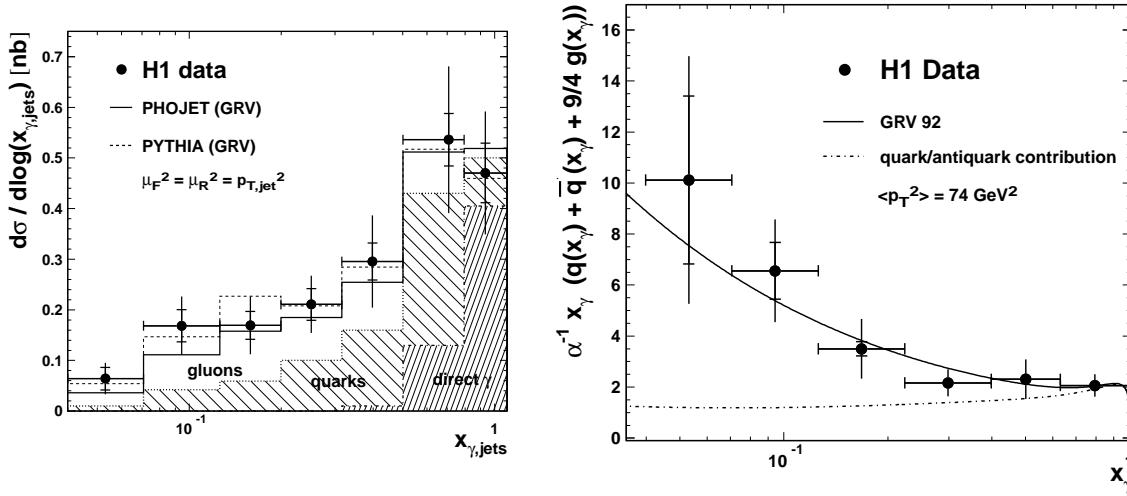


Figure 4: *Left*: The di-jet cross section as a function of the parton momentum fraction x_{γ}^{jet} . The histograms represent a LO QCD calculation showing the contributions of the direct photon-proton interactions as well as the quark and gluon induced processes using GRV pdfs for both photon and proton. *Right*: The x_{γ} dependence of the effective parton density of the real photon extracted from di-jet photoproduction; the curves superimposed are the expectation from QCD LO GRV92 parametrisation of photon structure.

we show the parton density in the photon extracted from the differential cross section. x_{γ}^{jet} has been unfolded to parton level x_{γ} and the effective parton density is determined by the comparison of MC and the data

$$f_{\gamma}^{DATA} = f_{\gamma}^{MC} \frac{\sigma^{DATA}}{\sigma^{MC}}. \quad (5)$$

Figure 5 shows the gluon content of the photon obtained from the effective photon pdf by subtraction of the GRV quark contribution. A good agreement with the gluon density derived from the photoproduction of high transverse momentum charged particles [19] should be noted, as these two measurements have different systematics. Thus the large gluon component of the photon pdf at low values of x_{γ} may be considered as established. The systematic errors dominate above $x_{\gamma} \approx 0.1$, but for low x_{γ} values the statistical errors are still important and in principle it is still possible to reach better precision at low x_{γ} .

Figures 4 and 5 show that at least some parametrisations of the photon pdf constrained by e^+e^- measurements are compatible with jet photoproduction in ep as calculated in LO. We can consider this fact as a demonstration of e^+e^-ep universality of the photon structure, but taking into account the large errors involved, at the semi-quantitative level only.

4.2 Measurement of the effective parton density of the virtual photon

One can study the structure of virtual photons in a similar way to that described in the previous section. Such a study [20] is presented in Figure 6 (left), based on sample of 6 pb^{-1} of DIS events in the kinematic range $1.6 \leq Q^2 \leq 80 \text{ GeV}^2$, $0.1 \leq y \leq 0.7$ with at least 2 jets with average squared transverse energy $\bar{E}_t^2 > 30 \text{ GeV}^2$. Jets are restricted to be asymmetric in energy, and the constraints are such that neither jet has $E_T \leq 4 \text{ GeV}$ and the sum is always $\geq 11 \text{ GeV}$.

In Figure 6 (left) the di-jet cross section is plotted as a function of x_{γ}^{jets} for different regions of Q^2 and E_T^2 . One sees a clear excess over the expectation of direct photon reactions, indicating that virtual photons also have a resolved part. The direct interactions are manifest in the region of $x_{\gamma}^{jets} \rightarrow 1$. With increasing Q^2 at fixed E_T^2 the direct contribution increases while the resolved is significant only for $E_T^2 > Q^2$ i.e. when the spatial extent of the photon exceeds the resolution of the probe. This is a beautiful demonstration of QFT at work.

It should be noted that pQCD does not provide a full theoretical description of the virtuality dependence of the parton density in the photon. There is only an asymptotic prediction [26] in LO for $F_2^{\gamma^*}$ i.e.

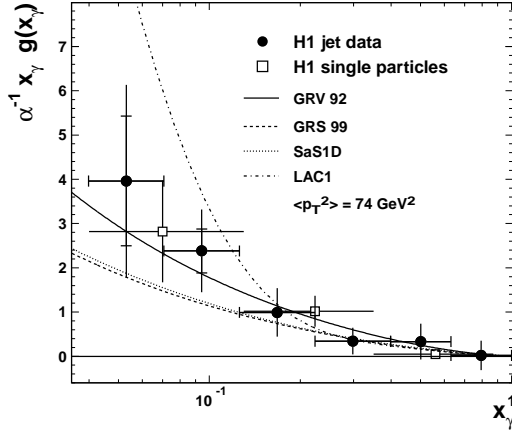


Figure 5: Gluon distribution $g(x_\gamma)$ of the photon as a function of the photon momentum fraction for a mean $\hat{p}_t^2 = 74 \text{ GeV}^2$ of hard partons. The inner error bars give statistical error and outer error bars give the total error. The data points with open squares show a previous measurement [19] of H1 which used single high E_T particles to determine the LO gluon density of the photon at a mean $\hat{p}_t^2 = 38 \text{ GeV}^2$. The leading order parametrisations of the gluon distribution based on fits to e^+e^- two-photon data are also shown.

the structure function of the virtual photon γ^*

$$F_2^\gamma = 3 \sum_q e_q^4 \frac{\alpha}{\pi} x [x^2 + (1-x)^2] \ln \frac{Q^2}{P^2}, \quad (6)$$

valid for $Q^2 \gg P^2 \geq \Lambda^2$. Here P^2 is the photon virtuality while Q^2 is the virtuality of the probe (resolution scale). The formula (6) is analogous to (1) for a quasi-real photon. Now, kinematics provides its own cut-off P^2 as long as it exceeds Λ^2 . The “hadron piece” in formula (1) no longer counts as $F_2^{VDM} \propto 1/P^4$,²

For the description of the triple differential di-jet cross section we can employ phenomenological models of the dependence of the effective parton density in the photon on its virtuality Q^2 [27], [29], [28]. The Drees-Godbole model (DG) [27] starts with parton densities in the real photon and suppresses them by a factor \mathcal{L}

$$\mathcal{L}(Q^2, E_T^2, \omega^2) = \frac{\ln \frac{E_T^2 + \omega^2}{Q^2 + \omega^2}}{\ln \frac{E_T^2 + \omega^2}{\omega^2}}, \quad (7)$$

where ω is a free parameter. The quark densities in the real photon are suppressed by \mathcal{L} and the gluon densities by \mathcal{L}^2 . This ansatz, based on analysis in [29], is designed to interpolate smoothly between $\ln(Q^2)$ and $\ln(Q^2/P^2)$ in the LO asymptotic formulae for real (1) and virtual (6) photons. In the model of Schuler and Sjöstrand [28], the perturbative anomalous component of the parton density in a virtual photon is designed to approach the asymptotic result (6) as in the DG model, while the VDM part is rapidly suppressed by the factor $m_V^2/(m_V^2 + Q^2)$. In this approach the parton density in a quasi-real photon has to be initially decomposed into perturbative and non-perturbative components, so that the description of the Q^2 suppression of the photon pdf is inseparable from the parametrisation of the quasi-real photon pdf. This is not the case for the DG model, which can be applied to any quasi-real photon pdf.

In Figure 6 (left) the predictions of the HERWIG MC with GRV photon pdf multiplied by the DG factor are compared with the data. Clearly the data are well described by the MC with suitable choice of the parameter $\omega = 0.2$ which controls the onset of the Q^2 suppression.

²Note that formulae (1) and (6) refer to the photon structure function as measured in e^+e^- experiments, and there are conflicting notations: in e^+e^- Q^2 always denotes the virtuality of the probe (i.e. resolution scale) while in ep experiments at HERA Q^2 traditionally denotes the virtuality of the photon which here happens to be a target. Throughout the article we stick to traditional notations, leaving the reader to determine the correct recognition of the symbols.

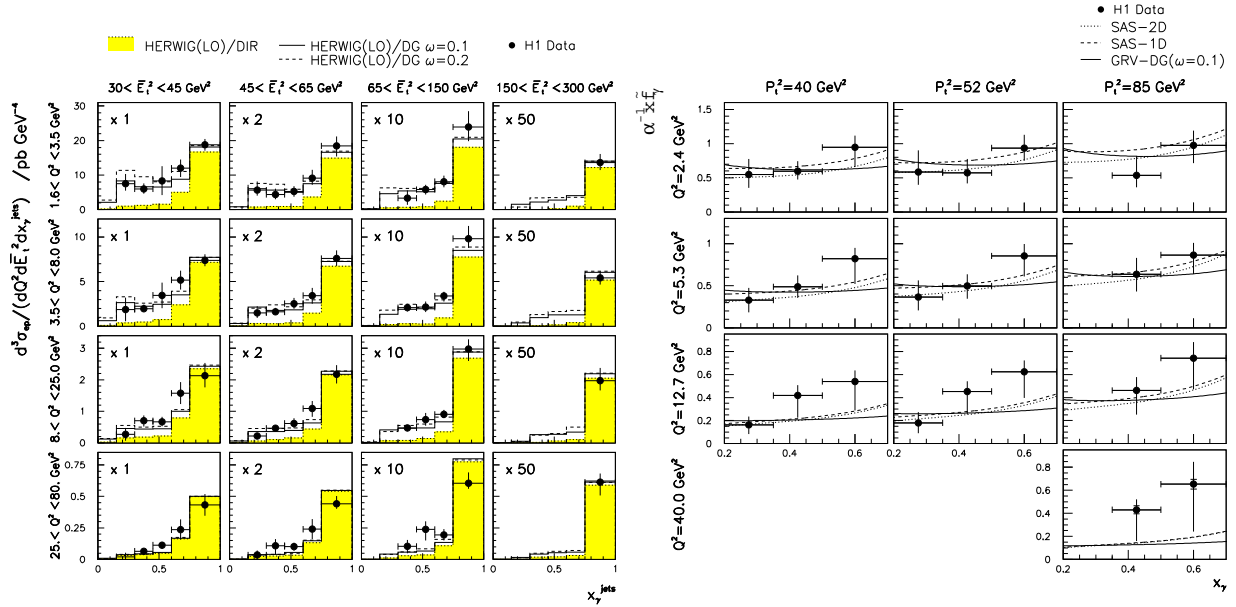


Figure 6: *Left*: The differential di-jet cross section $d^3\sigma_{ep}/dQ^2 d\bar{E}_t^2 dx_\gamma^{jets}$ as a function of x_γ^{jets} for different regions of \bar{E}_t^2 and Q^2 . The scale factors applied to cross sections are indicated. The error bar shows the quadratic sum of systematic and statistical errors. The absence of data point indicates that no measurement was made because of insufficient statistics for the two dimensional unfolding. Also shown is the HERWIG(LO)/DG model with 10% soft-underlying event and two choices of the Q^2 suppression factor ω . The full histogram is for $\omega = 0.1$ GeV and dashed for $\omega = 0.2$ GeV. The direct component is shown as a shaded histogram. *Right*: Leading order effective parton distribution function of virtual photons extracted from triple differential cross section on the left. The data are compared to several theoretical predictions explained in the text.

In Figure 6 (right) we show the effective parton density of the virtual photon extracted from the triple differential di-jet cross section (on the left). In the whole measurement range the systematic errors dominate the total error. The x_γ dependence of the effective parton density shows a tendency to rise with increasing x_γ as predicted by formula (6). For quasi-real photons in a similar x_γ range the pdf is flat. This fact can be interpreted as the effect of the VDM contribution, which preferentially fills out the low x_γ region flattening the otherwise rising x_γ -dependence of the anomalous pQCD contribution. With rising Q^2 , the VDM contribution rapidly decreases, leaving only the rising x_γ -dependence. The errors on the experimental data are clearly too large to differentiate between SAS and DG, although only SAS has a rising tendency for reasons explained before (the DG model has no explicit VDM component). In Figure 7 (left) we show the extracted photon pdf as a function of Q^2 . The data are compared with the pure VDM prediction and the DG and SAS models discussed above. The DG and SAS parametrisations describe the data up to $Q^2 \approx 25$ GeV². The last data point $25 \leq Q^2 \leq 80$ GeV² is above both parametrisations. This is however the region where $Q^2 \rightarrow E_T^2$ and non-leading terms not accounted for in the models are expected to be important and may affect the extraction of the effective parton distribution from the data (breakdown of factorisation).

The ZEUS collaboration investigated the photon pdf suppression with increasing Q^2 in a different way. They use an operational definition of direct and resolved di-jet cross sections: $\sigma^{dijet}(\text{direct}) = \sigma^{dijet}(x_\gamma^{jet} > 0.75)$, $\sigma^{dijet}(\text{resolved}) = \sigma^{dijet}(x_\gamma^{jet} < 0.75)$. In Figure 7 (right) we show the ratio of the so-defined “resolved” to “direct” contributions as a function of Q^2 . The SAS prediction is below the data points, but the shape of the dependence is correct.

At the end of this section we would like to underline that there is no basic difficulty in the theoretical description of the region $E_T^2 \approx Q^2$. On the contrary, in this region of phase space, terms with $\ln(E_T/Q)$

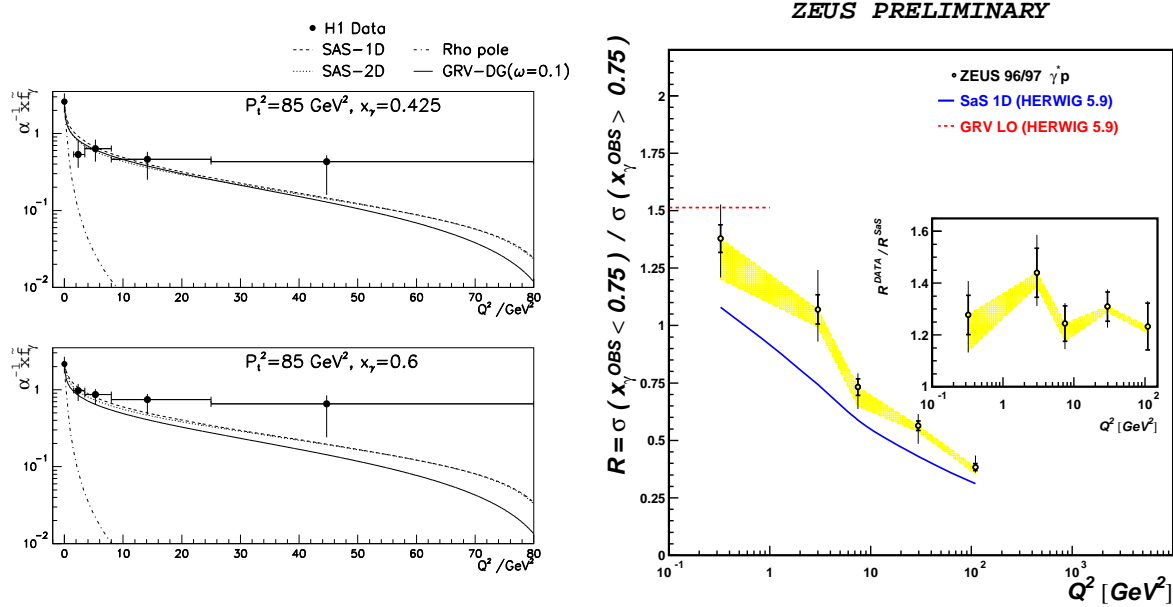


Figure 7: *Left:* The leading order effective parton density of the photon as a function of Q^2 for $E_T^2 = 85 \text{ GeV}^2$ and two values of x_γ . Also shown are predictions from the DG model using GRV-LO pdf for a real photon (solid line) and the SAS model (dotted line). The dot-dashed curve shows the photoproduction data scaled by a ρ -pole factor. *Right:* The ratio of di-jet cross sections, $R^{DATA} = \sigma(x_\gamma^{OBS} < 0.75) / \sigma(x_\gamma^{OBS} > 0.75)$ as a function of photon virtuality Q^2 . The points represent ZEUS data. The predictions of HERWIG MC, $R^{SAS} = \sigma(x_\gamma^{OBS} < 0.75) / \sigma(x_\gamma^{OBS} > 0.75)$ using the SAS 1D photon pdfs, are shown as a full line. The ratio R^{DATA} / R^{SAS} as a function of Q^2 is also shown in the inset.

appearing in the perturbative expansion are small, so that even fixed order theory is applicable in this case. It is only the photon structure function approach which breaks down for $Q \approx E_T$. Let us also note that in the range $E_T^2 \gg Q^2 \gg \Lambda^2$ the photon structure approach can, in principle, be replaced by resummed $(\ln(E_T^2)/Q^2)^n$ theory, because for the photon, unlike for hadrons, the purely perturbative (anomalous) part of pdf dominates completely at high values of E_T^2 . In this sense the structure function of the virtual photon could and should be considered as a convenient parametrisation of higher order QCD corrections which are not available yet.

5 Comparison of the measured di-jet cross section with a NLO QCD calculation

The ZEUS Collaboration analysis of di-jet photoproduction [23], [22], based on a large sample of events, confronts a precision measurement with a NLO QCD calculation. The cut on the transverse energy of jets $E_T^{jet1,2} > 14, 11 \text{ GeV}$ is so high that corrections for hadronisation and the soft underlying event are certainly small (less than 10%). Therefore the data, corrected only for detector effects, are compared directly to NLO QCD calculations [24] at the parton level. There is good general agreement of the di-jet cross section with the NLO calculation as seen e.g. in Figure 8 where it is plotted as a function of the transverse energy. While $E_{Tleading}^{jet}$ increases from 14 to 50 GeV, cross section falls by 3 orders of magnitude and no obvious deviations from theory are seen, except for events with forward jets $1 < \eta_{1,2}^{jet} < 2$ and $E_{Tleading}^{jet} < 25 \text{ GeV}$. Let us note that the theory-data discrepancy appears exactly in the region where the distance between “direct” and “direct + resolved” points is large, meaning that the influence of the resolved component is large. This tendency of the data becomes even more evident when the di-jet

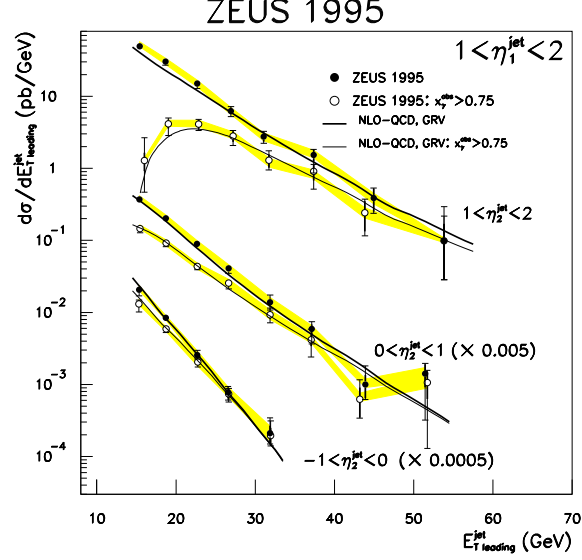


Figure 8: Di-jet cross section as a function of E_T^{jet1} for η_1^{jet} between 1 and 2 and several bins of η_2^{jet} . The filled circles correspond to the entire range while open circles correspond to “direct” events with $\gamma^{jet} > 0.75$. The data are compared to NLO-QCD calculations, using the GRV-HO parametrisation for the photon structure.

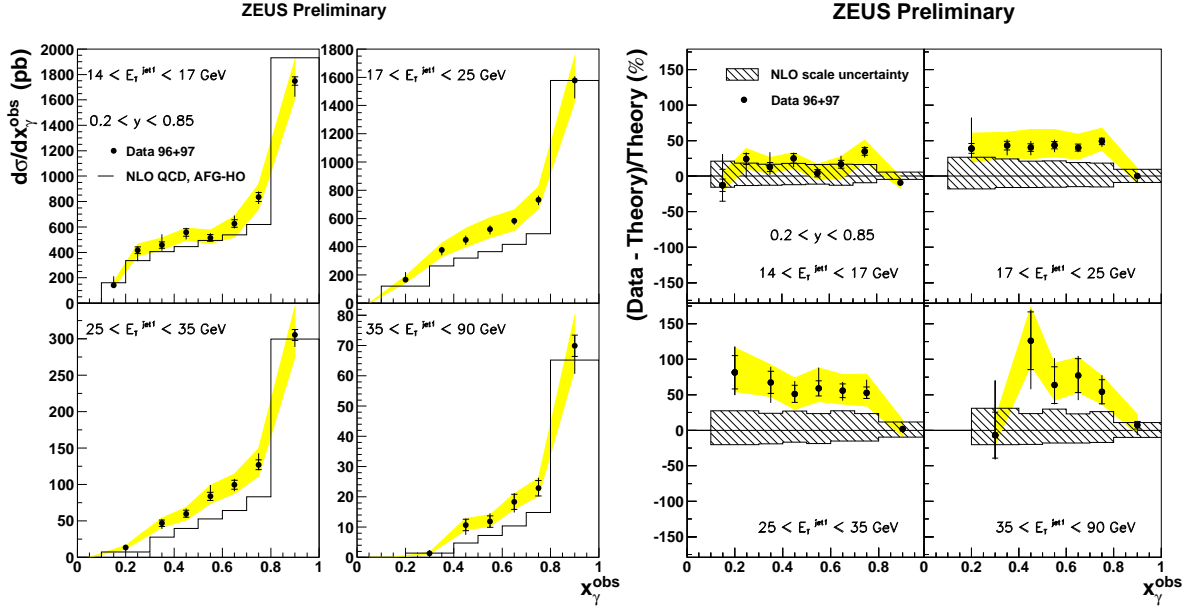


Figure 9: *Left*: Differential cross sections in x_γ^{obs} in slices of the transverse energy of the leading jet E_T^{jet1} . The data points are shown with statistical errors (inner bars) and statistical and systematic errors added in quadrature (outer bars). The scale uncertainty is shown as the shaded band. The data are compared to a NLO prediction which uses the AFG-HO photon structure function. *Right*: The relative difference in cross sections between data and NLO predictions for distributions in the Figure on the left. The estimation of the scale uncertainty in the NLO calculation, obtained by varying the factorisation and renormalisation scales by a factor two, is shown as the diagonally shaded band.

cross section is plotted as a function of the photon momentum fraction [23]. In Figure 9 (left) the di-jet cross section is plotted as a function of $x_\gamma^{obs} \equiv x_\gamma^{jet}$ in several bins of the transverse energy of the leading jet. Except for the last bin (dominated by direct process) all data points are above the NLO cross section.

Figure 9 (right) shows the relative value of the theory-data discrepancy as a function of x_γ^{obs} . The relative discrepancy reaches 60%. Even taking into account the uncertainty of the theory due to the choice of the NLO scale (shown as shaded area) and the experimental uncertainty due to the hadronic energy scale, we have to admit that there is an indication that the parton densities in the photon are underestimated. Incidentally, this conclusion seems to be confirmed by recent measurements of the di-jet cross section in $\gamma^*\gamma^*$ collisions [15]. Even so it is difficult to accept without reservation that the pdf in photon is much underestimated. The argument against such interpretation of ZEUS and OPAL results is the general good agreement of the LEP measurements of photon structure function with GRV parametrisation. This problem certainly deserves further scrutiny.

6 Summary and Conclusion

Measurements of $e\gamma$ DIS and jet electroproduction at HERA confirm the simple picture of photon structure first identified in e^+e^- experiments at PETRA. There is general compatibility of e^+e^- and ep measurements which demonstrates the validity of a factorisable structure which can be assigned to the photon, both real and virtual. Properties of the photon structure function are in agreement with theoretical expectations, in particular its dependence on the photon momentum fraction and resolution scale. Also the parton density suppression with increasing photon virtuality is in agreement with phenomenological models based on asymptotic QCD predictions.

The recent precision measurements of the di-jet cross section seem to indicate that the existing parametrisations (based on e^+e^- measurements) of the photon pdf are inadequate for a precise description of the data using NLO theory. This problem certainly deserves further scrutiny.

The accumulated LEP, LEP2 and HERA data with much reduced systematic uncertainties over a very wide kinematic range now wait for a combined analysis, which would result in a new NLO parametrisation of the photon pdf. The concepts and tools for such an analysis have yet to be developed.

References

- [1] J. Dainton, Invited presentation at the discussion meeting *The Quark Structure of Matter*, Royal Society, London, May 24 2000, to appear in Philosophical Transactions of the Royal Society of London Series A: Mathematical, Physical and Engineering Sciences, [hep-ex/0009033].
- [2] M. Krawczyk, A. Zembruski and M. Staszal, *Survey of Present Data on Photon Structure Functions and Resolved Processes* to appear in *Phys. Rep.*, [hep-ph/0011083].
- [3] R. Nisius, *The photon structure from deep inelastic electron-photon scattering*, [hep-ex/9912049].
- [4] A. Levy, *The proton and the photon, who is probing whom in electroproduction?* [hep-ph/0002015].
- [5] G. Abbiendi et al. (OPAL Collaboration), *Eur. Phys. J. C* **18** (2000) 15.
- [6] M. Melles, *Nucl. Phys. B (Proc. Suppl.)* **82** (2000) 379.
- [7] B.L. Ioffe, *Phys. Lett. B* **30** (1969) 123; B.L. Ioffe, V.A. Khoze and L.N. Lipatov, *Hard Processes*, (North-Holland, 1984).
- [8] J.J. Sakurai, *Phys. Rev. Lett.* **22** (1969) 981.
- [9] E. Witten, *Nucl. Phys. B* **120** (1977) 189.
- [10] G. Altarelli, G. Parisi, *Nucl. Phys. B* **126** (1977) 298.
- [11] H. Abramowicz, K. Charchula and A. Levy, *Phys. Lett. B* **269** (1991) 458.
- [12] M. Gluck, E. Reya and A. Vogt, *Phys. Rev. D* **46** (1992) 1973.
- [13] P. Aurenche, J.P. Guillet and M. Fontannaz, *Zeit. Phys. C* **64** (1994) 621.
- [14] G.A. Schuler and T. Sjöstrand, *Nucl. Phys. B* **407** (1993) 539.
- [15] T. Wengler, *The hadronic picture of the photon*, Proceedings of 30th International Conference on High Energy Physics (ICHEP 2000), Osaka.
- [16] T. Ahmed et al (H1 Collab.), *Nucl. Phys. B* **445** (1995) 195.
- [17] C. Adloff et al (H1 Collab.), *Phys. Lett. B* **415** (1997) 418.

- [18] C. Adloff et al (H1 Collab.), *Europ. Phys. J.* **C1** (1999) 97.
- [19] C. Adloff et al (H1 Collab.), *Europ. Phys. J.* **C10** (1999) 363.
- [20] C. Adloff et al (H1 Collab.), *Europ. Phys. J.* **C13** (2000) 397.
- [21] J. Breitweg et al (ZEUS Collab.), *Europ. Phys. J.* **C11** (1999) 35.
- [22] J. Breitweg et al (ZEUS Collab.), *Europ. Phys. J.* **C6** (1999) 67.
- [23] ZEUS Collab., *The Structure of the Photon and the Dynamics of Resolved Photon Processes in Di-jet Photoproduction at HERA*, Proceedings of 30th International Conference on High Energy Physics (ICHEP 2000), Osaka.
- [24] M. Klasen, T. Kleinwort and G. Kramer, *Europ. Phys. J.* **C1** (1998) 1.
- [25] B.V. Combridge and C.J. Maxwell, *Nucl. Phys.* **B239** (1984) 429.
- [26] T. Uematsu and T.F. Walsh, *Nucl. Phys.* **B199** (1982) 93.
- [27] M. Drees and R. Godbole, *Phys. Rev.* **D50** (1994) 3124.
- [28] T. Sjöstrand and G.A.Schuler, *Phys. Lett.* **B376** (1996) 193.
- [29] F. Borzumati and G.A. Schuler, *Zeit. Phys.* **C58** (1993) 139.